

Numerical investigations on the ergodic properties of two coupled Pomeau-Manneville maps

Matteo Sala^a, Cesar Manchein^{b,c}, Roberto Artuso^{c,d}

^aMax Planck Institute for the Physics of Complex Systems, Nöthnitzer Straße 38, 01187 Dresden (Germany);

^bDepartamento de Física, Universidade do Estado de Santa Catarina, 89219-710 Joinville, (Brazil);

^cCenter for Nonlinear and Complex Systems and Dipartimento di Scienza e Alta Tecnologia, Via Valleggio 11, 22100 Como (Italy);

^dI.N.F.N., Sezione di Milano, Via Celoria 16, 20133 Milano (Italy)

Abstract

We present extensive numerical investigations on ergodic and mixing properties of a map of the unit square defined by two identical Pomeau-Manneville maps interacting via a diffusive linear coupling. In spite of the anomalous features of the system, such as the coexistence of stretched exponential and power-law decays for the dynamical indicators under study, we find interesting regular dependences on both the intermittency and the coupling parameter, which pave the way for further, possibly analytical, developments. In particular we find that, for arbitrarily small coupling, the statistics of Poincaré recurrences deviates from the single-map distribution to a power-law decay with exactly twice the single-map anomalous exponent; this also suggests a conjecture for higher dimensional systems.

Keywords: intermittency, coupled maps, recurrence times, Lyapunov exponents

1. Introduction

Intermittent systems represent a paradigmatic example of *weak chaos*, where a chaotic sea coexists with regular, non chaotic structures. Popular examples of such a situation involve area preserving maps (see for example [1]), where regular structures often occupy a finite fraction of the whole phase-space; on the other side, systems having a *zero-measure* source of non-hyperbolicity often allow more quantitative considerations: in this respect Pomeau-Manneville maps [2] represent an outstanding example, where many peculiar properties (from power-law correlation decay, to generalised central limit theorems, to infinite ergodic theory), have been anticipated by Gaspard and Wang [3, 4] and later discussed and proved in several papers, with also remarkable applications to the problem of anomalous transport. Here we address the important problem of multi-dimensional extension of such prototypical models by *diffusively* coupling a pair of Pomeau-Manneville maps: it is not trivial, indeed, how the increased dimensionality may modify the dynamical properties, *e.g.* allowing the system to avoid or deform the intermittent behaviour. Apart from the intrinsic interest, this study represents a natural preliminary step towards many-dimensional extensions, which have been proposed, for example, as the proper framework to study the statistics of genomic sequences [5]. The paper is organized as follows: Section 2 describes some general properties of the 1D Pomeau-Manneville map and its 2D version coupled via the diffusive scheme; stability arguments allow to identify and avoid the so-called synchronization regime. In Section 3 we present the numerical results about filling rates, Poincaré recurrences and finite-time Lyapunov exponents. Finally, Section 4 summarizes the main results of the paper.

Email addresses: msala@pks.mpg.de (Matteo Sala), cesar.manchein@udesc.br (Cesar Manchein), roberto.artuso@uninsubria.it (Roberto Artuso)

2. General setting

2.1. Pomeau-Manneville Map

The Pomeau-Manneville map is the transformation defined on the unit-interval $f_z : [0, 1] \rightarrow [0, 1]$, $1 < z \in \mathbb{R}$, as:

$$\begin{aligned} x \mapsto f_z(x) &= x + x^z \pmod{1} \\ &= x + x^z - \chi_z(x), \end{aligned} \quad (1)$$

where $\chi_z(x)$ is the *characteristic function* of the set $[\xi, 1]$ with $\xi(z) < 1$ being defined by $f_z(\xi) = 1$. Dynamical properties of the map are determined by the indifferent fixed point at $x = 0$, where the dynamics is slowed down by the tangency (see figure 1), and they strongly depend on the *intermittency parameter* z . When $z > 2$ there is no invariant probability measure (the invariant density close to the origin goes as x^{1-z}) and the map (1) provides an example of *infinite ergodicity* [6, 7, 8]; we will not consider such a case in the present paper. Indeed, in the regime $1 < z < 2$ the map is ergodic and the invariant measure close to the origin has the same behavior as before (but now the singularity is integrable). For such intermittency parameter values the map is also mixing, with polynomially decaying correlation functions: the corresponding power-law exponent Γ (such that asymptotically the mixing speed is $n^{-\Gamma}$) can be expressed in terms of the intermittency parameter as follows [4, 9]:

$$\Gamma = \frac{1}{z-1} - 1. \quad (2)$$

Notice that, when $z \geq 3/2$, correlations are not integrable: a striking dynamical manifestation of this observation is that Birkhoff sum converge to a Lévy stable law, *i.e.* we have a generalised central limit theorem [10].

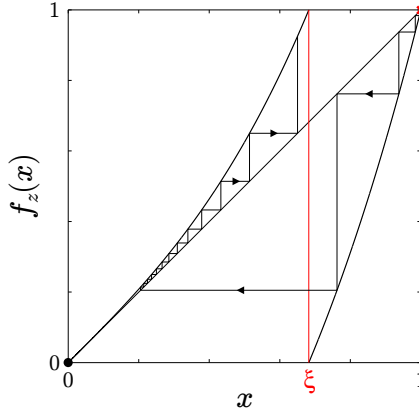


Figure 1: Pomeau-Manneville map for $z = 3$ and $\xi(z) \simeq 0.6823$, along with a typical orbit: after being quickly repelled away from the unstable fixed point at $x = 1$ (red cross) and being reinjected into $[0, \xi]$, it slowly escapes from the indifferent fixed point at $x = 0$ (black dot). The nearer the reinjection is to $x = 0$, the longer the escape lasts; the slowing down depends on the *strength* of the tangency through the intermittency parameter z .

2.2. Diffusive Coupling

We start our analysis by considering two identical copies of map (1) acting on the unit square $S := [0, 1] \times [0, 1]$:

$$\mathbf{f}_z : \begin{bmatrix} x \\ y \end{bmatrix} \mapsto \begin{bmatrix} f_z(x) \\ f_z(y) \end{bmatrix}; \quad (3)$$

and, by coupling them via the linear transformation \mathbf{M}_ε which depends on the coupling parameter $\varepsilon \in [0, 1/2[$:

$$\mathbf{M}_\varepsilon = \begin{bmatrix} 1 - \varepsilon & \varepsilon \\ \varepsilon & 1 - \varepsilon \end{bmatrix} \Rightarrow \mathbf{f}_{z,\varepsilon}(\mathbf{x}) := \mathbf{M}_\varepsilon \circ \mathbf{f}_z(\mathbf{x}), \quad (4)$$

we obtain a two-parameters map $\mathbf{f}_{z,\varepsilon}$, so called *diffusively coupled*, whose components now read:

$$\mathbf{f}_{z,\varepsilon} : \begin{bmatrix} x \\ y \end{bmatrix} \mapsto \begin{bmatrix} f_z(x) + \varepsilon(f_z(y) - f_z(x)) \\ f_z(y) - \varepsilon(f_z(y) - f_z(x)) \end{bmatrix}. \quad (5)$$

By defining \mathbf{X} as the exchange map $(x, y) \rightarrow (y, x)$, one can show that the coupled map $\mathbf{f}_{z,\varepsilon}$ then satisfies the relations:

$$\begin{aligned} \bullet \mathbf{X} \circ \mathbf{f}_{z,\varepsilon} &= \mathbf{f}_{z,\varepsilon} \circ \mathbf{X} \\ \bullet \mathbf{f}_{z,1-\varepsilon} &= \mathbf{X} \circ \mathbf{f}_{z,\varepsilon} \end{aligned} \quad \Rightarrow \quad \mathbf{f}_{z,1-\varepsilon}^n = \mathbf{X}^n \circ \mathbf{f}_{z,\varepsilon}^n = \begin{cases} \mathbf{f}_{z,\varepsilon}^{2m} \\ \mathbf{X} \mathbf{f}_{z,\varepsilon}^{2m+1} \end{cases}, \quad (6)$$

from which we deduce that $\mathbf{f}_{z,\varepsilon}$ is *invariant* under the exchange $(x, y, \varepsilon) \rightarrow (y, x, 1 - \varepsilon)$, and the cases ε and $(1 - \varepsilon)$ are thus equivalent. Most importantly, we notice that the action of map $\mathbf{f}_{z,\varepsilon}$ is not surjective on the whole unit square S , but it maps S into the rhombus-shaped subset K (see figure 2), as the following map sequence shows:

$$\mathbf{f}_{z,\varepsilon} : S \xrightarrow{\mathbf{f}_z} S \xrightarrow{\mathbf{M}_\varepsilon} K \subset S; \quad (7)$$

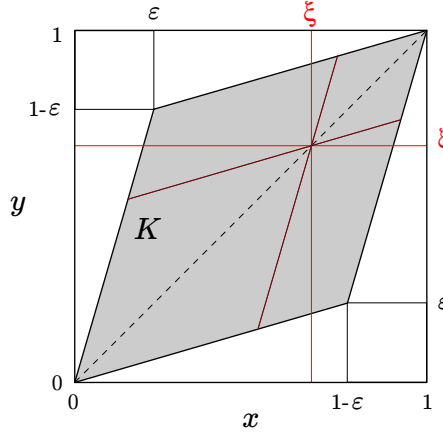


Figure 2: The linear transformation \mathbf{M}_ε from equation (4) squeezes the unit square S into the gray kite $K \subset S$; this implies that the areas outside K can never be reached from points in S , suggesting to employ the modified map as in equation (8). Notice that the diagonal of S is an invariant set.

this property suggests to consider instead a surjective version of map (5), by defining coordinates $\tilde{\mathbf{x}} = \mathbf{M}_\varepsilon^{-1} \mathbf{x}$:

$$\tilde{\mathbf{f}}_{z,\varepsilon}(\tilde{\mathbf{x}}) = \mathbf{f}_z(\mathbf{M}_\varepsilon \tilde{\mathbf{x}}) \quad \Rightarrow \quad \tilde{\mathbf{f}}_{z,\varepsilon} : \begin{bmatrix} \tilde{x} \\ \tilde{y} \end{bmatrix} \mapsto \begin{bmatrix} f_z(\tilde{x} + \varepsilon(\tilde{y} - \tilde{x})) \\ f_z(\tilde{y} - \varepsilon(\tilde{y} - \tilde{x})) \end{bmatrix}; \quad (8)$$

This is the map we consider in all of our numerical experiments, motivated by the well-definedness of Poincaré recurrences and by the fact that, due to the invertible change of coordinates, the two maps (5) and (8) are completely equivalent. By the fact that $x = \tilde{x} + \varepsilon(\tilde{y} - \tilde{x})$ and $y = \tilde{y} - \varepsilon(\tilde{y} - \tilde{x})$, the *Jacobian matrix* associated to map (8) reads:

$$\mathbf{J}(\tilde{\mathbf{x}}) = \begin{bmatrix} f'_z(x) & 0 \\ 0 & f'_z(y) \end{bmatrix} \begin{bmatrix} 1-\varepsilon & \varepsilon \\ \varepsilon & 1-\varepsilon \end{bmatrix} \quad \Rightarrow \quad \begin{aligned} \det \mathbf{J}(\tilde{\mathbf{x}}) &= (1-2\varepsilon) f'_z(x) f'_z(y) \\ \text{trace } \mathbf{J}(\tilde{\mathbf{x}}) &= (1-\varepsilon)(f'_z(x) + f'_z(y)) \end{aligned}; \quad (9)$$

since the unit square diagonal is an *invariant set* for both versions of the map (we may call it the *synchronised* state of the system), it is informative to study its stability properties. For points $\mathbf{x} = (x, x)$, indeed, the first/second eigenvector of \mathbf{J} is respectively parallel/orthogonal to the diagonal itself. Simple calculations show that, for any point on the diagonal, the two Lyapunov exponents can be written as:

$$\lambda_1 = \lambda^{1D}, \quad \lambda_2 = \lambda^{1D} + \ln(1-2\varepsilon) < \lambda_1; \quad (10)$$

where λ^{1D} is the Lyapunov exponent of the 1D Pomeau-Manneville map (1); it is known (see for example [11]) that, when the coupling ε is sufficiently strong, λ_2 becomes negative, turning the diagonal into an attractor and leading to global synchronization [12, 13] (that is, the system synchronizes for any initial condition in the unit square S). By setting $\lambda_2 = 0$, the critical value ε_{cr} for the coupling parameter above which synchronisation appears can be obtained:

$$\varepsilon_{cr} = \frac{1 - e^{-\lambda^{1D}}}{2}, \quad (11)$$

and it depends on parameter z through the exponent λ^{1D} ; this relation holds for any pair of diffusively coupled, identical 1D maps. In what follows we will only consider cases in which $\varepsilon \ll \varepsilon_{cr}$, *i.e.* far away from synchronisation regimes; this can be easily achieved by a preliminary estimate of the 1D Lyapunov exponent λ^{1D} for the chosen value of z (we remark once again that, in the z range we are considering, the Lyapunov exponent λ^{1D} is always positive).

3. Numerical Results

3.1. Ergodicity Test: Filling Rate

To check ergodicity, we use the method discussed in [14], namely we partition the phase-space into N cells (here a regular square grid with $N = 2000 \times 2000$) and consider, for a long trajectory, the indicator:

$$Q_N(n) = \frac{\text{number of unvisited cells up to the } n\text{-th iteration}}{N}; \quad (12)$$

a numerical verification of ergodicity is equivalent to checking that such a function vanish in the long time limit, independently of how fine we choose the phase-space partition (*i.e.* in the large N limit). In figure 3, panel (a), it is shown how indeed we get convergence to zero of $Q_N(n)$ in a typical simulation (the orbit eventually visits all the cells of the grid). Apart from the qualitative confirmation of ergodicity, it is interesting to consider the way in which $Q_N(n)$ vanishes, since, for models of fully chaotic dynamics, it is expected to decay as a simple exponential [14] $Q_N(n) \sim e^{-n/N}$. While generalisations of such a decay have been proposed [15], we remark that in [16] a pure exponential decay has been observed, despite the model under investigation is a billiard table shaped like a fully irrational triangle, a system with very weak ergodic properties. In our simulations we never get any evidence of such a simple asymptotics, while the data are fitted by stretched exponentials, with stretching exponent φ and prefactor C :

$$Q_N(n) \sim e^{-C \cdot n^\varphi}; \quad (13)$$

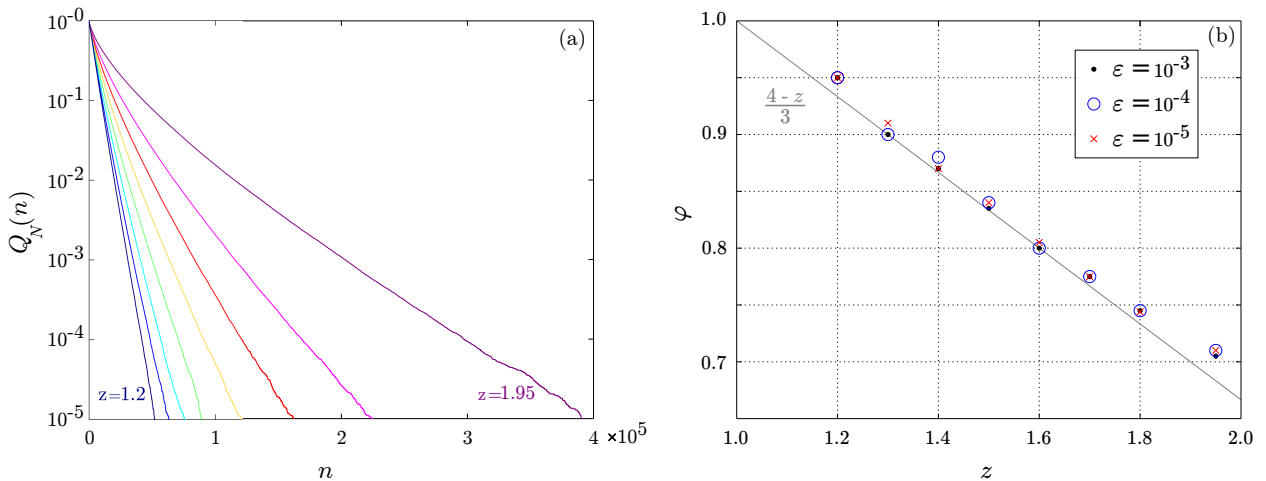


Figure 3: Panel (a): stretched exponential decay of $Q_N(n)$ (fraction of unvisited cells at time n) for the values of intermittency exponent $z = 1.2, 1.3, 1.4, 1.5, 1.6, 1.7, 1.8, 1.95$ (respectively from left- to right-most graph) at coupling parameter $\varepsilon = 10^{-4}$; the total number of cells $N = 2000 \times 2000$ is eventually visited, but the plot is truncated at $Q_N(n) = 10^{-5}$ for clarity. Panel (b): the stretching-exponent φ from equation (13) as a function of z for the three coupling parameters $\varepsilon = 10^{-3}, 10^{-4}, 10^{-5}$; in all three cases the almost linear trends are close to the line $(4 - z)/3$ (in grey, for reference), leading to pure exponential at $z = 1$ (*i.e.* the Bernoulli map limit).

the resulting exponents are plotted in figure 3, panel (b), showing an almost linear dependence w.r.t. the intermittency parameter z , independent of the coupling parameter ε ; indeed, the latter turns out to have influence only on the exponent prefactor C (not shown), a property shared also by the other two dynamical indicators we consider below. Stretched exponential relaxations have sound physical relevance (see for example [17, 18]); in the present context a possible interpretation is like follows: stretched exponential decays, with anomalous exponent β and inverse characteristic time λ^* , may be viewed as a continuous superposition of purely exponential decays [19]:

$$e^{(\lambda^* n)^\beta} = \int_0^\infty ds e^{-s \lambda^* n} P(s, \beta), \quad (14)$$

where $P(s, \beta)$ represents the distribution of weights for each value of the exponential rate s . We found that a similar decomposition arises in the generalization of the random model investigated in [15], where, once the ‘greyness’ parameter is introduced for the cells partitioning the phase-space (such ‘greyness’ can be understood as the *density of the measure*, essentially encoding the number of cells having the same *a priori* probability to be visited, albeit defined in the $N \rightarrow \infty$ limit), the following expression for the filling rate is obtained:

$$Q_N(n) = \int_0^1 dg e^{-ag n/N} w(g), \quad (15)$$

where ag is the average occupancy number in a cell of ‘greyness’ g , and $w(g)$ is the probability distribution of g over the full set of cells. The numerical distributions $w(g)$, obtained from orbit densities on the same 2000×2000 cells grid used for filling rates, are shown for a single ε value in figure 4, panel (a); in the inset, a qualitative comparison with examples of $P(s, \beta)$ from equation (14) suggests some connection between the two families of distributions. In spite of that, in figure 4, panel (b), we check that such connection, if present, is not trivial: by fitting the power-law right-tails of the ‘greyness’ distributions $w(g)$ and using the corresponding asymptotics for $P(s \rightarrow \infty, \beta) \sim 1/s^{\beta+1}$ as in equation (14) of [19], we find that the effective β values fall outside the range allowed by $P(s, \beta)$, which is $\beta \in [0, 1]$. Notice that the best-fits in figure 4, panel (b), giving $\beta \rightarrow \infty$ as $z \rightarrow 1$ are consistent with the fact that the right-tail of $w(g)$ becomes *exponential* (i.e. no finite power-law exponent exists) when $z = 1$.

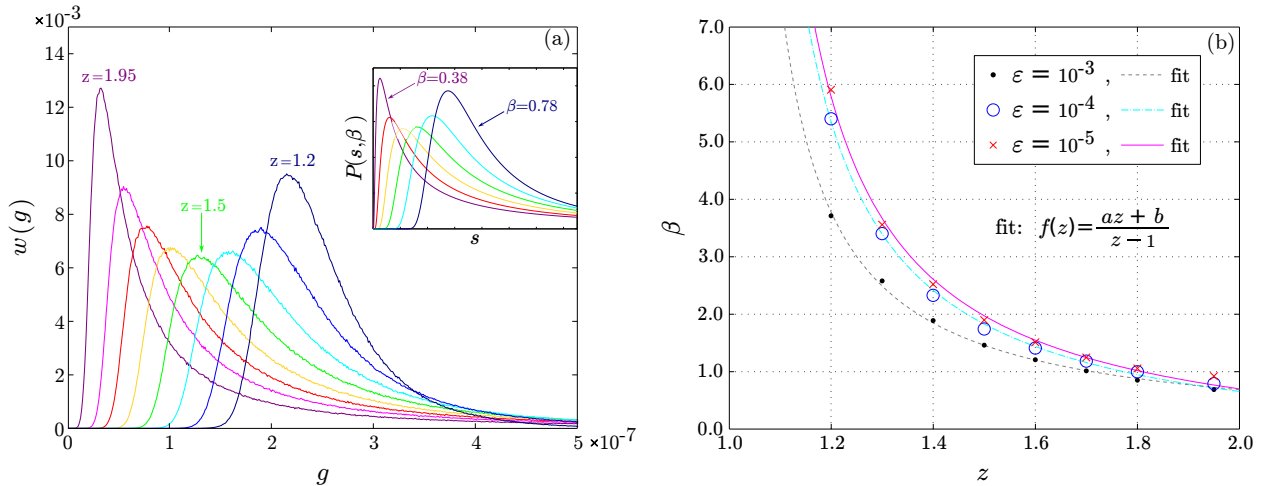


Figure 4: Panel (a): probability distributions $w(g)$ for the number of cells having the same occupancy density, or, ‘greyness’ g (here from single orbits of length 10^9 over a square grid of 2000×2000 cells) for the same parameters of panel (a) in figure 3; in the inset, examples of distributions as in equation (14), whose connection with $w(g)$, in spite of the similarity, is still missing. Panel (b): the effective power-law exponents β from the right-tails of $w(g)$ as a function of z for the three values $\varepsilon = 10^{-3}, 10^{-4}, 10^{-5}$; these fall far outside the allowed range $\beta \in [0, 1]$, proving that $w(g)$ cannot be fitted by $P(s, \beta)$. The curves are best-fits, giving $\beta \rightarrow \infty$ as $z \rightarrow 1$ in agreement with the exponential decay of $w(g)$ at $z = 1$.

3.2. Mixing Test 1: Recurrence Times

It is well known that direct numerical indications of mixing are extremely hard to attain for non trivial systems [20]: tests that proved to be numerically stabler involve either statistics of Poincaré recurrences [21, 22, 23, 24] or large

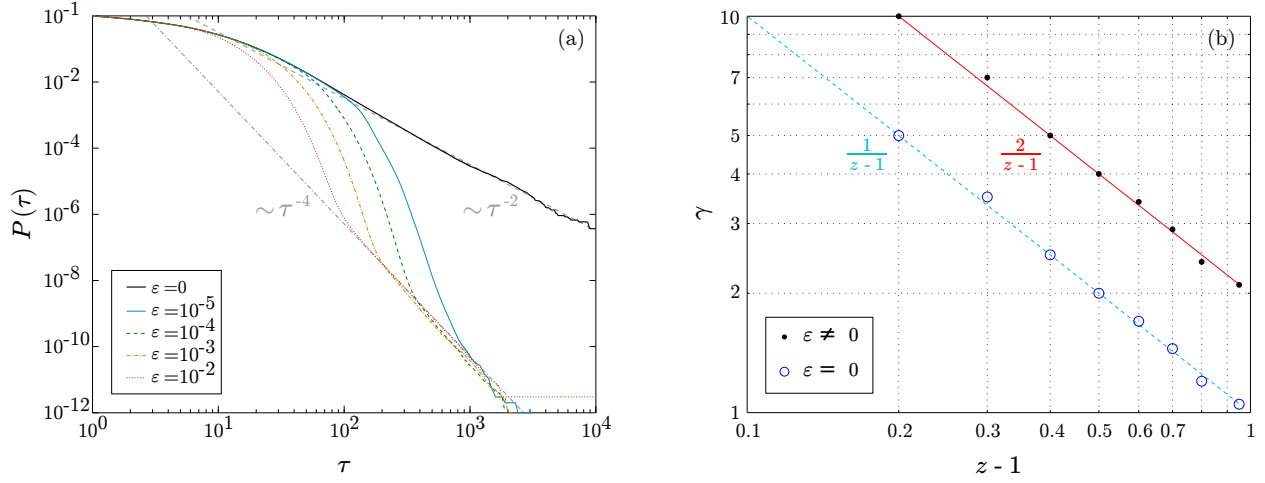


Figure 5: Panel (a): examples of cumulative probability for recurrence times at $z = 1.5$ at coupling parameter $\varepsilon = 10^{-2}, 10^{-4}, 10^{-5}, 0$; dashed and dash-dotted lines are fits to the power-law decay of respectively the $\varepsilon = 0$ and $\varepsilon \neq 0$ cases. Panel (b): the same power-law exponents for the set of intermittency exponents under study $z = 1.2, 1.3, 1.4, 1.5, 1.6, 1.7, 1.8, 1.95$; we find the same exponents for all $\varepsilon \neq 0$ cases (black dots, continuous red line $\sim 2/(z-1)$ for reference), and all of them coincide with *twice* the $\varepsilon = 0$ exponents (blue circles, dashed light-blue line $\sim 1/(z-1)$ for reference). Notice that the characteristic escape-time at which the power-law tails begin is larger as the coupling parameter $\varepsilon \rightarrow 0$.

deviations for Birkhoff sums [25]. In this subsection we present simulations for the statistics of Poincaré recurrences in a fixed box in phase space: we choose $(x, y) \in [0.10, 0.55] \times [0.55, 1.00]$ avoiding the diagonal (synchronised states), and run a set of 10^{12} trajectories initialized inside the box. We remark that such a huge ensemble of trajectories is essential to detect the probability of very long recurrences. To visualise the data we plot the cumulative probability $P(\tau) := P(t_{rec} \geq \tau)$ for the orbit to return in the box only *after* a certain time τ : if the cumulative probability decays polynomially with an exponent γ , then we expect [21, 22, 23] that also correlations display a power law decay, with an exponent $\Gamma = \gamma - 1$. By such analysis, in figure 5 we confirm the presence of an asymptotic power-law decay:

$$P(\tau) \sim \tau^{-\gamma} \quad (16)$$

whose exponent γ depends on the intermittency parameter z but not on the diffusive coupling ε . As illustrated in figure 5, panel (b), such dependence for $\varepsilon \neq 0$ coincides with *twice* the exponent behaviour for the case $\varepsilon = 0$, that

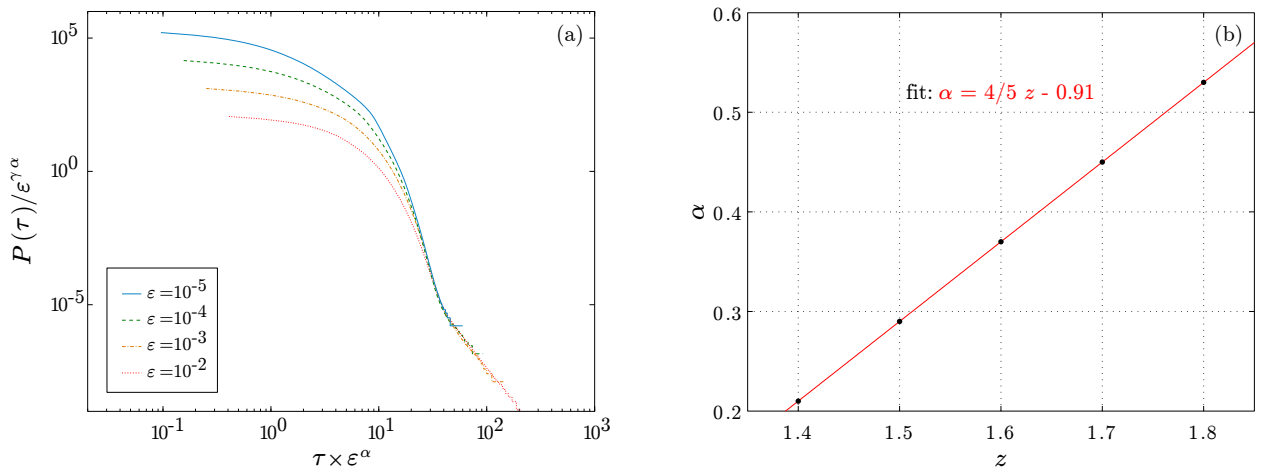


Figure 6: Panel (a): cumulative probability of recurrence times at $z = 1.5$ (same as in figure 5, panel (a)) after rescaling according to equation (17). Panel (b): the rescaling exponent α as a function of parameter z for the cases in which the curve collapse is apparent; the solid red line is a linear fit.

is $\gamma(z) \sim 1/(z-1)$, namely the exponent of the $1D$ map (see [26] for an early derivation of such a formula, based on escape rates from the indifferent fixed point). This suggests, that at least asymptotically, *any* non-zero coupling induces uncorrelated behaviour on the two maps return probabilities; nevertheless the deviation from the uncoupled distribution (figure 5, panel (a), thick solid curve) takes place at longer return-times as the coupling parameter ε is reduced (figure 5, panel (a), thin curves). The coupling parameter ε influences only the pre-asymptotic decay, suggesting the existence of a scaling law: indeed (see figure 6, panel(a)) we find it by writing $P(\tau)$ in the form:

$$P(\tau) \sim \varepsilon^{\gamma\alpha} \mathcal{F}(\tau\varepsilon^\alpha); \quad (17)$$

where γ is the power-law decay exponent, α is a fitting parameter and \mathcal{F} is a function independent on ε : an appropriate choice of α allows to get curve collapsing in the asymptotic power-law regime; in figure 6, panel (b), the plot of α as a function of the intermittency parameter z shows a behavior that is quite accurately reproduced by a linear fit with slope $\sim 4/5$.

3.3. Mixing Test 2: Finite Time Lyapunov Exponents

An alternative indirect way of probing mixing speed is provided by large deviation analysis of the largest finite-time Lyapunov exponents: this method is based upon rigorous results, proved in [27, 28] (see also [29]), and it was numerically tested on intermittent and Hamiltonian systems in [25]. Since it is a less widely used technique with respect to scrutinizing the statistics of Poincaré recurrences, we briefly recall how it works operationally: for further details see [25]. The crucial quantity to take into account is the probability distribution of finite-time Lyapunov exponents $\mathcal{P}_n(\lambda)$ (leading expansion rates up to some fixed time n) which, for an ergodic system, collapses to a Dirac delta in the $n \rightarrow \infty$ limit. The idea [27, 28, 29] is that, by fixing a threshold $\tilde{\lambda} < \lambda_\infty$ (λ_∞ being the asymptotic largest Lyapunov exponent) one can define:

$$\mathcal{M}_{\tilde{\lambda}}(n) = \int_0^{\tilde{\lambda}} d\lambda \mathcal{P}_n(\lambda), \quad (18)$$

such that (in a large deviation philosophy) the way $\mathcal{M}_{\tilde{\lambda}}(n)$ decays as $n \rightarrow \infty$ should also rule the mixing speed. The result is independent on the choice of threshold $\tilde{\lambda}$ as long as it is below the asymptotic λ_∞ ; however, in numerical implementations one has to make preliminary checks to fix the threshold reasonably (not too close to λ_∞ to spoil statistics, not too small to have only few points in the tail). The procedure we follow here (not knowing *a priori* the invariant measure) is to follow a single trajectory for 10^{12} time steps and reconstruct $\mathcal{P}_n(\lambda)|_{n \leq 10^6}$ from 10^6 consecutive chunks of trajectory: the threshold is then fixed depending on the goodness of the collected statistic. In figure 7, panel (a) we find that, like in the case of filling rates, the data are best fitted by a stretched exponential decay $\mathcal{M}_{\tilde{\lambda}}(n) \sim e^{-C \cdot n^\sigma}$;

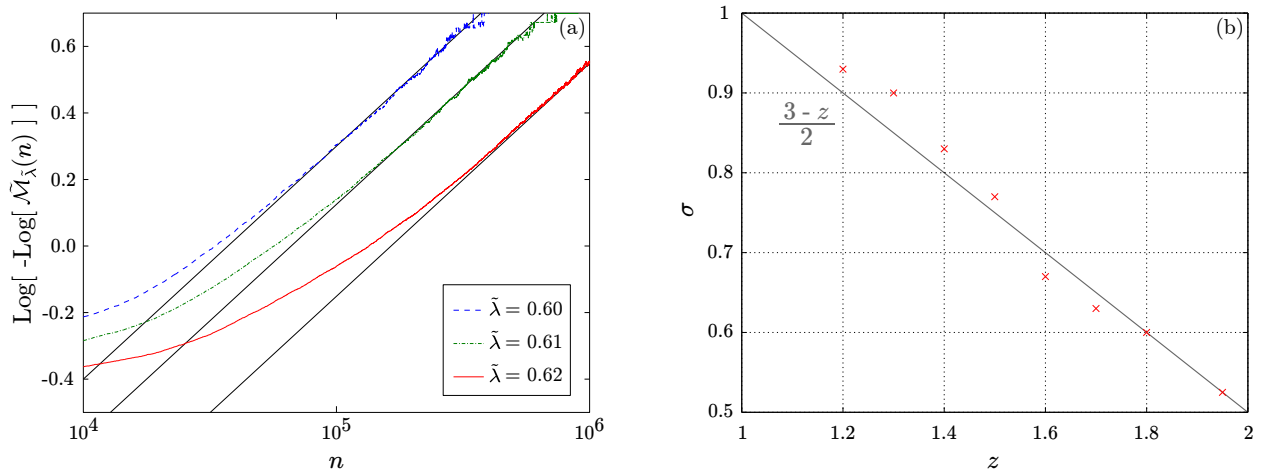


Figure 7: Panel (a): examples of stretched exponential fits for the decay of $\tilde{\mathcal{M}}_{\tilde{\lambda}}(n) := \mathcal{M}_{\tilde{\lambda}}(n)/\mathcal{M}_{\tilde{\lambda}}(0)$ (*i.e.* equation (18) normalized w.r.t. $n = 0$ for fitting purposes) for parameters $z = 1.5$, $\varepsilon = 10^{-5}$ and three different values of $\tilde{\lambda}$; notice that the stretching exponent is the same for all three cases, but the exponential prefactors are not. Panel (b): the stretching exponent σ as a function of z at $\varepsilon = 10^{-5}$; the straight line is for reference.

notice that different values of $\tilde{\lambda}$ give the same stretching-exponent σ but different prefactors C . We find that the exponent σ , at diffusive coupling $\varepsilon = 10^{-5}$, display a roughly linear dependence on parameter z (figure 7, panel (b)). Finally, we remark that the discrepancy between the stretched exponential for the $\mathcal{M}_{\tilde{\lambda}}(n)$ integral and the power-law decay for Poincaré recurrences definitely deserves further studies, since, in principle, the two should be related.

4. Conclusions

We have investigated the ergodic properties of two diffusively coupled, identical Pomeau-Manneville maps. In particular we have characterized how single trajectories fill fine partitions of the phase space: this yields an indication of ergodicity, with a nontrivial filling rate in the form of a stretched exponential. The same time-law appears in the decay of sub-threshold finite-time Lyapunov exponent distribution, which probes the speed of mixing; by contrast, a polynomial decay is instead observed when the mixing rate is explored by considering the statistics of Poincaré recurrences. In addition, the latter display a power-law exponent which is exactly twice the one for the single Pomeau-Manneville map, suggesting some kind of asymptotic independence between the two coordinates. Supported by preliminary results on three diffusively coupled Pomeau-Manneville maps [30], we conjecture that the same mechanism holds in a multi-dimensional setting, leading to N -times the $1D$ power-law exponent for a system of N coupled maps.

Acknowledgments

CM thanks CNPq for financial support. We are grateful to Bastien Fernandez for the insightful discussions on intermittent and diffusively coupled maps.

References

- [1] Zaslavsky GM. Chaos, fractional kinetics and anomalous transport. *Phys.Rep.* 2002; 371:461-580.
- [2] Pomeau Y, Manneville P. Intermittent transition to turbulence in dissipative dynamical systems. *Commun.Math.Phys.* 1980; 74:189-97.
- [3] Gaspard P, Wang X-J. Sporadicity: between periodic and chaotic dynamical behaviors. *Proc.Natl.Acad.Sci. USA* 1988; 85:4591-5.
- [4] Wang X-J. Statistical physics of temporal intermittency. *Phys.Rev. A* 1989; 40:6647-61.
- [5] Provata A, Beck C. Coupled intermittent maps modelling the statistics of genomic sequences: a network approach. *Phys.Rev. E* 2012; 86:046101.1-9
- [6] Aaronson J. An introduction to infinite ergodic theory. Providence:AMS; 1997.
- [7] Zweimüller R. Ergodic properties of infinite measure preserving interval maps with indifferent fixed points. *Ergod. Th. & Dynam. Sys.* 2000;20:1519-49.
- [8] Bel G, Barkai E. Weak ergodicity breaking with deterministic dynamics. *Europhys.Lett.* 2006;74:15-21.
- [9] Hu H. Decay of correlations for piecewise smooth maps with indifferent fixed points. *Ergod. Th. & Dynam. Sys.* 2004;24:495-524.
- [10] Gouëzel S. Central limit theorem and stable laws for intermittent maps. *Probab. Th. and Rel.Fields.* 2004;128:82-122.
- [11] Pikovsky AS, Grassberger P. Symmetry breaking bifurcation for coupled chaotic attractors. *J.Phys. A.* 1991;24:4587-97.
- [12] Pikovsky A, Rosenblum M, Kurths J. Synchronization. A universal concept in nonlinear sciences. Cambridge:CUP; 2001.
- [13] Boccaletti S, Kurths J, Osipov, G, Valladares DL, Zhou CS. The synchronization of chaotic systems. *Phys.Rep.* 2002;366:1-101.
- [14] Robnik M, Dobnikar J, Rapisarda A, Prosen T, Petrovšek M. New universal aspects of diffusion in strongly chaotic systems. *J.Phys. A.* 1997;30:L803-13.
- [15] Prosen T, Robnik M. General Poissonian model of diffusion in chaotic components. *J. Phys. A.* 1998;31:L345-53.
- [16] Casati G, Prosen T. Triangle map: a model of quantum chaos. *Phys.Rev.Lett.* 2000;85:4261-4.
- [17] Phillips JC. Stretched exponential relaxation in molecular and electronic glasses. *Rep.Progr.Phys.* 1996;59:1133-1207.
- [18] Laherrère J, Sornette D. Stretched exponential distributions in nature and economy: “fat tails” with characteristic scales. *Europ.Phys.J.* 1998;2:525-39.
- [19] Johnstone DC. Stretched exponential relaxation arising from a continuous sum of exponential decays. *Phys.Rev. B.* 2006;74:184430.1-7
- [20] Artuso R. Correlation decay and return time statistics. *Physica D.* 1999;131:68-77.
- [21] Channon SR, Lebowitz JL. Numerical experiments in stochasticity and heteroclinic oscillation. *Ann. NY Acad.Sci.* 1980;357:108-18.
- [22] Chirikov BV, Shepelyansky DL. Correlation properties of dynamical chaos in Hamiltonian systems. *Physica D.* 1984;13:395-400.
- [23] Artuso R, Casati G, Guarneri I. Numerical experiments on billiards. *J. Stat.Phys.* 1996;83:145-66.
- [24] Artuso R, Cavallasca L, Cristadoro G. Dynamical and transport properties in a family of intermittent area-preserving maps. *Phys.Rev. E.* 2008;77:046206.1-9
- [25] Artuso R, Manchein C. Instability statistics and mixing rates. *Phys.Rev. E.* 2009;80:036210.1-.5.
- [26] Geisel T, Thomae S. Anomalous diffusion in intermittent chaotic systems. *Phys. Rev. Lett.* 1984; 52:1936-39.
- [27] Melbourne I. Large and moderate deviations for slowly mixing dynamical systems. *Proc. Amer. Math. Soc.* 2009;137:1735-41.
- [28] Pollicott M, Sharp R. Large deviations for intermittent maps. *Nonlinearity.* 2009;22:2079-82.
- [29] Alves JF, Luzzatto S, Pinheiro V. Lyapunov exponents and rates of mixing. *Ergod. Th. & Dynam. Sys.* 2004;24:637-57.
- [30] In preparation.